Hydrothermal equalibria and ore formation

Alekseyev V.A., Medvedeva L.S., Sedykh E.M., Gromyak I.N. Silica separation in closed quartz-water-vapor system as a result of distillation

Vernadsky Institute of Geochemistry and Analytical Chemistry RAS, Moscow

Abstract. Under a small horizontal temperature gradient (0.1 grad/cm), an equilibrium quartz-water system transforms into non-equilibrium one. This is expressed as a precipitation of metastable opal above the meniscus at the expense of a decrease in aqueous silica concentration. A process of distillation explains such separation. Mathematical model of the process in agreement with the experimental data was elaborated. Under real conditions with temperature gradient, the distillation can go on in systems of any composition. In this case, solution composition cannot be predicted on the basis of only thermodynamic and kinetic data.

Key words: quartz, water, equilibrium violation, temperature gradient, preferential evaporation, meniscus edge, distillation.

Previous investigations. The interaction of quartz with water at 300ºC usually leads quickly to the achievement of chemical equilibrium, i.e., to a saturation of water with silica (fig. 1A). Since under these conditions quartz is stable mineral [Dove, 1995], a further increase in time does not change the pattern. We had such result also but only in a half of our experiments. In the rest of the experiments after the attainment of equilibrium, the system moved away from it (fig. 1B and 1C). We conducted the experiments using ampoule-quenched method in standard vertical electric furnaces with Al blocks where autoclaves were inserted in pairs, one on another. It turned out that the unusual silica behavior showed itself only in the lower autoclaves and only when the upper autoclaves were absent [Alekseyev, Medvedeva, 2013a]. On this basis we proposed that initial reason of different silica behavior was difference in temperature gradient.
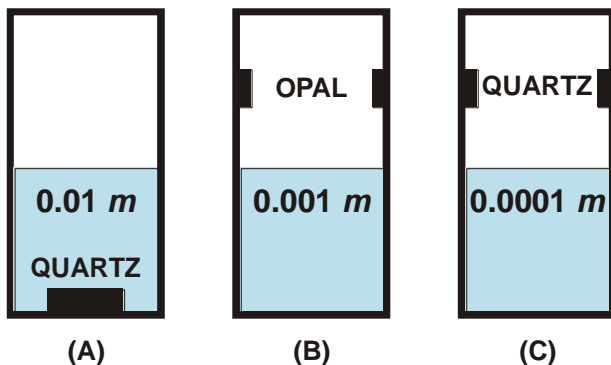

Fig. 1. Stages of unusual silica behavior in closed quartz-water system at 300°C [Alekseyev et al., 2013; Alekseyev, Medvedeva, 2013a]. (A) – Saturation of liquid water with silica with respect to quartz (chemical equilibrium). (B) – Quartz disappearance in liquid water, metastable opal appearance in vapor phase, and the decrease of silica concentration in liquid water by an order of magnitude. (C) – Transformation of opal into secondary quartz and the decrease of silica concentration in liquid water by an order of magnitude once more.

Temperature gradient was measured on the autoclave surface on two opposite sides at various heights with ten Chromel-Alumel flexible thermocouples. To decrease accidental and systematic errors of temperature measurements, the following procedures were applied: 1) Al cover plates with concave surface for hot ends (good thermal contact), 2) thermal isolation of cold ends (temperature equalization), 3) aging of thermocouples during long (months) heating at 300ºC, 4) selection of the most stable thermocouples, 5) determination of the corrections for thermocouple readings using Pb melting point (327.4ºC), 6) immersion of thermocouples in the furnace to the same depth. These measurements have shown that intensification of the unusual silica behavior is related to the increase in absolute values of horizontal temperature gradient (fig. 2). The influence of temperature gradient on the reaction of mineral dissolution is usually expressed through temperature dependence of its solubility and dissolution rate. At small temperature difference, these quantities are little affected, then, the influence of temperature gradient is ignored. In our case, small temperature difference radically alters the system.
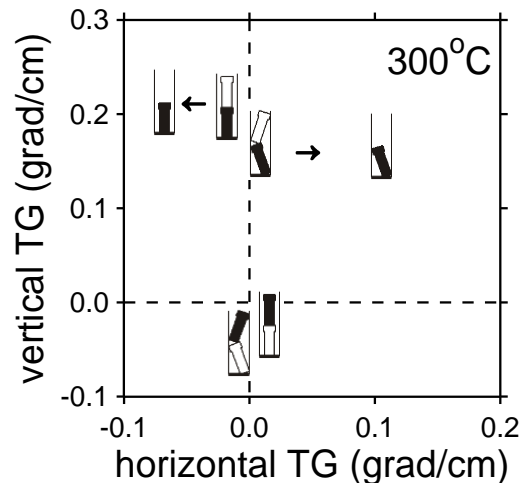

Fig. 2. Average temperature gradient (TG) on the autoclave surface on the level of ampoule position (0 – 6 cm from the bottom). Symbols show mutual positions of measured autoclave (solid symbol) and another autoclave (open symbol) if it exists in the hole of Al block situated in the electric furnace. Arrows show the displacement of temperature gradients in the lower autoclaves after the removal of the upper autoclaves, i.e., under activation of the unusual silica behavior.

Mechanism. We performed the estimation of the greatest possible body of hypotheses to explain the unusual silica behavior [Alekseyev et al., 2013; Alekseyev, Medvedeva, 2013a]. The hypothesis for the preferential evaporation at the meniscus edge is the most likely. This process is well known for open non-equilibrium system with wall heating, i.e., under temperature gradient [Panchamgam et al., 2008]. We believe that it operates in closed equilibrium system also. Then, preferential evaporation at the meniscus edge must be compensated by preferential condensation at the meniscus center to retain the balance of the overall fluxes of evaporation and condensation. As a result of operation

of these two local processes, distillation must take place, i.e., gradual substitution of condensate with low silica concentration for water with high silica concentration. We elaborated a simple mathematical model of such substitution and divided the overall time into the multitude of small intervals Δt. The balance equation (1) describes silica concentration at the end of the first interval:

$$m_t = m_0 - (m_0 - m_v)JS\Delta t/M. \tag{1}$$

Here m_0 is the initial aqueous silica concentration in liquid water, m_v is the silica concentration in water vapor equal to 0.05 mmol/kg in equilibrium with quartz [Plyasunov, 2012], J is the specific rate of preferential evaporation, S is the surface area of the zone of preferential evaporation: $S = \pi dL$, where d is the ampoule diameter ($d = 1$ cm), L is the zone width ($L \approx 2$ μm [Panchamgam et al., 2008]), M is the water mass in the ampoule. The rate equation (2) takes into account additional quartz dissolution if it exists [Rimstidt, Barnes, 1980]:

$$m_t = m_0\exp(\Delta tk(S_q/M)/m_{eq}) + m_{eq}(1 - \exp(\Delta tk(S_q/M)/m_{eq})) \tag{2}$$

Here k is the dissolution rate constant (5.72×10^{-8} mol m^{-2} s^{-1}), S_q/M is the ratio of quartz surface area and water mass (m^2/kg), m_{eq} is the silica concentration in solution in equilibrium with quartz (0.01 mol/kg). Then the calculations were performed for subsequent time intervals. In doing so, the final concentration of the previous interval was equal to the initial concentration of the subsequent interval.

The peculiarity of this distillation process is that a circular cell involving two branches is formed at the water-vapor interface under the action of a small temperature gradient. The branch at the meniscus edge is directed upwards under the action of preferential evaporation. The branch at the meniscus center is directed downwards under the action of preferential condensation. The existence of this cell precludes the possibility of the establishment of chemical equilibrium between liquid and vapor water phases.
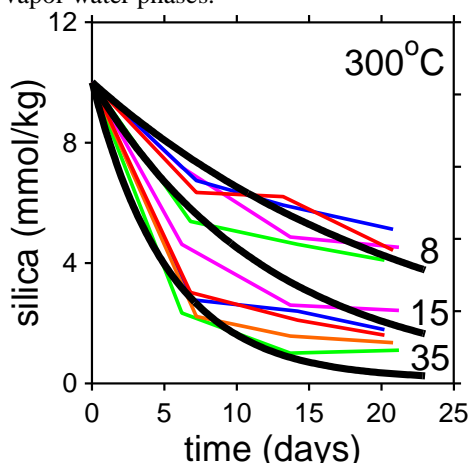
Experimental verification. The experiments were conducted using ampoule-quenched method [Alekseyev et al., 2013]. At first as a result of interaction of crushed quartz with water at 300°C, we obtained the solution saturated with respect to quartz (10 mmol/kg). Then this solution was overflowed into platinum ampoules (by 1 g), which were weld up hermetically and heated at 300°C in autoclaves situated in the lower parts of Al blocks in vertical electric furnaces. A fixed time later, the autoclaves were quenched in cold water, the solutions from the ampoules were filtered (pore size was 0.05μ), diluted with HCl solution (2 %), and analyzed for Si (ICP-AES).

The experiments have shown the decrease in aqueous silica concentration with time but the rate of this decrease varied in different holes of Al blocks (fig. 3). This is explained by uneven gap between Al block and a heater, i.e., by variation of temperature gradient. The modeling results agreed with experimental results at preferential evaporation rates of 8 to 35 g m^{-2} s^{-1} (fig. 3). These values constitute only about one part to million parts of the total equilibrium flux of evaporation-condensation calculated using equation for plane surface [Schrage, 1953].

In figure 4, the modeling results are compared with the results of experiments with quartz and water fulfilled earlier. The agreement of both the results is good if one takes into consideration that both the rate of preferential evaporation at the meniscus edge and the water mass were varied here. Horizontal parts of the curves in Fig. 4 correspond to steady states when the rate of silica removal from liquid water as a result of preferential evaporation at the meniscus edge and evaporate precipitation above the meniscus is equal to the rate of silica appearance as a result of quartz dissolution. The subsequent lowering of aqueous silica concentration takes place after quartz disappearance from liquid water. Minimum silica concentration in liquid water in the experiments is close to quartz solubility in water vapor. This is also testifies in favor of agreement of the model and the experiments.
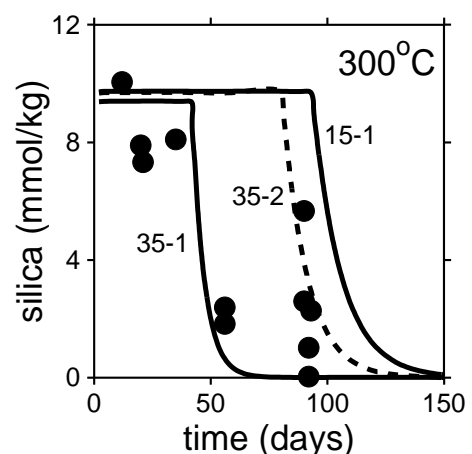

Fig. 3. Dependence of silica concentration on time in water with initial silica concentration of 10 mmol/kg (equilibrium with quartz). Colored broken lines show the experimental results in the lower autoclaves in different holes of Al blocks. Black curves show modeling results. Numbers at the curves denote the rate of preferential evaporation (g m^{-2} s^{-1}). Ampoule diameter is 1 cm, water mass is 1 g.

Fig 4. Time dependence of aqueous silica concentration in quarts-water system. Symbols show the results of experiments in the lower autoclaves [Alekseyev, Medvedeva, 2013a] recalculated for heating duration without the upper autoclaves. Numbers at the curves show the rate of preferential evaporation (the first number, g m^{-2} s^{-1}) and the water mass (the second number, g). $S_q/M = 6$ m^2/kg, the mass ratio of quartz and water is 0.005.

In figure 5, initial stage of quartz dissolution is shown at the presence and at the absence of distillation. It is followed from this figure that at low S_q/M values (in the experiments with single crystals), the distillation can influence significantly on the results of quartz solubility and dissolution rate measurement.

Because of its universality, the described distillation mechanism can exist in closed systems of any composition under experimental, technological, and natural conditions. In the case of its appearance, solution composition cannot be predicted on the basis of only thermodynamic and kinetic data. It is necessary to take into account solution dynamic also.
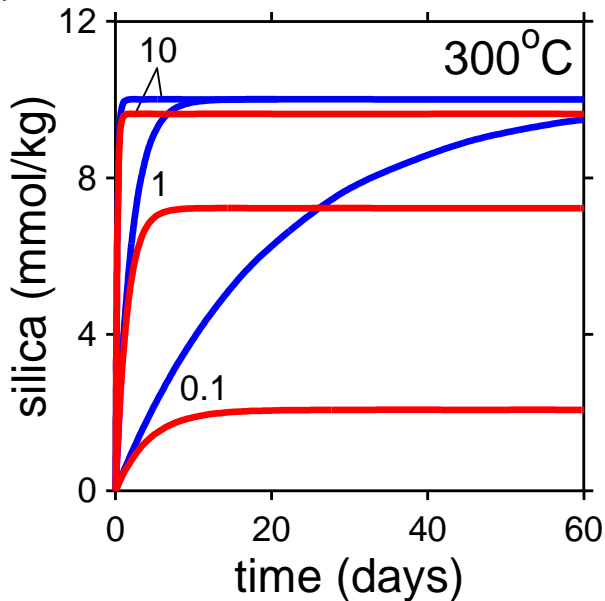

Fig. 5. Initial stage of quartz dissolution at the absence (blue lines) and at the presence (red lines) of the distillation process. The modeling results have shown for 1 g of water, $J = 35$ g m^{-2} s^{-1}, and for three values of S_q/M (m^2/kg).

References

1. Alekseyev, V.A., L.S. Medvedeva (2013a). Disturbance of thermodynamic equilibrium of the quartz-water system and silica separation from the liquid phase at a small temperature gradient. *Procedia Earth and Planetary Science.* V. 7. P. 6 – 9.
2. Alekseyev V.A., L.S. Medvedeva (2013b). Spontaneous violation of quartz-water chemical equilibrium: new data and revision of previous data. *Experimental Geochemistry.* V. 1. N 3. URL: http://exp-geochem.ru/JPdf/03_2013/ENG/03_03_2013_Eng.pdf
3. Alexeyev, V.A., L.S. Medvedeva, N.P. Starshinova (2013). Paradoxical transformation of the equilibrium quartz–water system into an unequilibrated one. *Geochemistry International.* V. 51, №. 5, pp. 382–404.
4. Dove, P. M. (1995). Kinetic and thermodynamic controls on silica reactivity in weathering environments. *Rev. Mineral.* V. 31, P. 235-290.
5. Panchamgam, S. S., A. Chatterjee, J. L. Plawsky, P. C. Jr. Wayner (2008). Comprehensive experimental and theoretical study of fluid flow and heat transfer in a microscopic evaporating meniscus in a miniature heat exchanger. *Int. J. Heat Mass Transfer.* V. 51, № 21-22, P. 5368-5379.
6. Plyasunov, A.V. (2012). Thermodynamics of Si(OH)$_4$ in the vapor phase of water: Henry's and vapor–liquid distribution constants, fugacity and cross virial coefficients. *Geochim. Cosmochim. Acta.* V. 77, P. 215-231.
7. Rimstidt, J. D., H. L. Barnes (1980). The kinetics of silica–water reactions. *Geochim. Cosmochim. Acta.* V. 44, № 11, P. 1683-1699.
8. Schrage, R.W. (1953) *A theoretical Study of Interphase Mass Transfer.* New York: Columbia University Press, Chap. 3.

Dadze T.P., Kashirtseva G.A., Novikov M.P., Plyasunov A.V. Experimental study of the MoO₃ solubility in aqueous HCl solutions at T=300°C and P=100 bar.

Institute of Experimental Mineralogy of RAS

Abstract. The solubility of MoO$_3$ was experimentally studied in aqueous HCl solutions at T=300°C and P=100 bar. The results showed a complex dependence of the solubility of MoO$_3$ on the HCl content. With the increase of the HCl molality from $5 \cdot 10^{-5}$ to 0.025 the molybdenum content in solution decreased from $1.4 \cdot 10^{-2}$ m to $9 \cdot 10^{-3}$ m, and the solutions were markedly acidified after the experiment. With a further increase of the acid concentration from 0.05 to 0.10 m, pH of the solutions does not change after the experiments, and the molybdenum content in the solution increases to 0.02m, which suggests the change of dominant complexes in solution under the given parameters.

Key words: Experiment, molybdenum trioxide, solubility, hydrothermal parameters, HCl solutions.

The purpose of this study was to investigate the solubility of crystalline MoO$_3$ in aqueous HCl solutions at T=300°C and P=100 bar. In order to conduct experiments, we obtained crystalline MoO$_3$ of a reactive purity by calcining ammonium molybdate [Korjakin, 1974] in three steps: 3 hours drying at 100-120°C, then calcining for 2 hours at 450°C and for three hours at 700°C. The obtained molybdenum trioxide was calcined at 550-580°C and then at 690-780°C for an additional purification and recrystallization of the amorphous component. The XRD analysis of the obtained material revealed the presence of only crystalline molybdenum trioxide.

Experiments were conducted in an autoclave made of titanium alloy VT-8, pre-passivated with 20% nitric acid at 400°C for one day. Autoclaves were placed in a gradient-free zone of a cylindrical vertical furnace. The temperature control was carried out using the thermostat Miniterm-300. Temperature fluctuations during the experiments were within ±2°C. The pressure in the autoclave was set by a filling coefficients using PVT-data for water. An accurately weighed load of a crystalline MoO$_3$ was placed in a titanium container which was suspended at the obturator in top of the autoclave. The quenching of autoclaves was carried out by running cold water for 5-7 minutes. The pH values of the HCl solutions before the experiment and after quenching were measured by an ion selective analyzer "EKOTEST-120". The time to reach equilibrium was determined experimentally (Fig. 1).
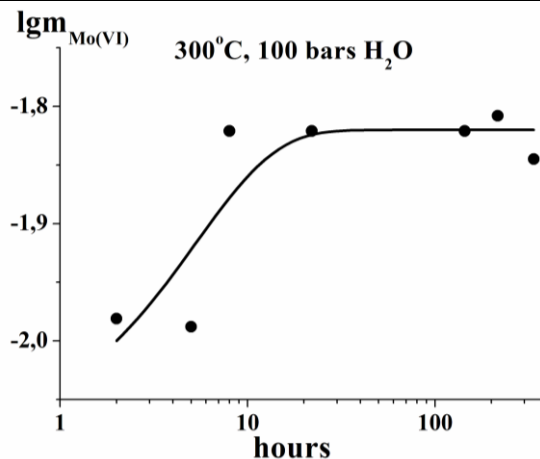
Fig. 1. The kinetics of dissolution of molybdenum trioxide.

The experimental results show that the equilibrium is reached in one day and do not contradict the literature data [Ivanova, 1975].

The composition of solid phases after runs was determined by the X-ray diffraction, which showed that after the experiments the solid phase was presented only by crystalline MoO_3. The concentration of molybdenum in solution after the experiment was determined colorimetrically using Specol-11 at $\lambda=453$ nm and duplicated by the weight loss (WL) method. A satisfactory agreements of the analytical and WL results on the concentration of molybdenum in solution should be noted (Fig. 2). Solutions after quenching, despite the high concentration of molybdenum, remained completely transparent and retained their stability for a long time. There was a significant acidification of the solutions after the experiments.

Results of the previous study of the solubility of MoO_3 in water and aqueous solutions of $HClO_4$ [Dadze, 2014] allowed us to assume that under the given conditions (T=300°C, P=100 bar) monomeric forms $H_2MoO_4^{\circ}$ and $HMoO_4^{-}$ are formed and the major factor is the acidity of the solution. However, data of the present study show a complex dependence of the solubility of MoO_3 on the concentration of aqueous HCl solutions (Fig. 2).
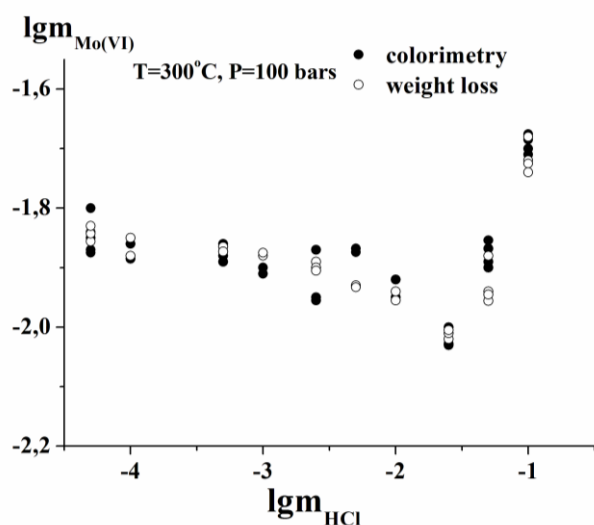

Fig.2. Dependence of the solubility of MoO_3 on the HCl concentration at T=300°C, P=100 bar.

With the increase of the HCl molality from $5 \cdot 10^{-5}$ to 0.025 the molybdenum content in solution decreased from $1.4 \cdot 10^{-2}$ m to $9 \cdot 10^{-3}$ m, and the solutions became markedly acidified after the experiment. With a further increase of the acid concentration from 0.05 to 0.10 m, pH of the solutions does not change after the experiments, and the molybdenum content in the solution increases to 0.02 m, which suggests the change of dominant complexes in solution under the given parameters. It should be noted that in the work [Rempel, 2008] on the investigation of the solubility of MoO_3 in the HCl-containing vapor phase, a dramatic increase of the Mo concentration with the increasing fugacity of HCl was also observed, which was explained by formation of the complex species MoO_2Cl_2.

References:

1. Koryakin Yu.V., Angelov I.I. (1974) Pure chemicals. M.: "Khimiya", 406 pp (in Russian).
2. Ivanova G.F., Levkina N.I., Nesterova L.A. and others. (1975) Equilibria in the system MoO3-H2O at temperatures 25-300 oC, Geokhimiya, № 2, p. 234-247.
3. Dadze T.P., Kashirtseva G.A., Novikov M.P., AV Plyasunov A.V., Shapovalov Yu.B. (2014) The solubility of MoO₃ in aqueous HClO4 solutions at T=300°C and P=100 bar (experimental data). DAN, v. 456, № 1, pp. 1-2. (in Russian).
4. Rempel K.U., Williams-Jones A.E., Migdisov A.A. (2008) The solubility of molybdenum dioxide and trioxide in HCl-bearing water vapour at 350oC and pressures up to 160 bars. Geochim. Cosmochim. Acta, v. 72. pp 3074-3083

Zagrtdenov[1] N.R., Bychkov[1,2] A.Y., Nikolaeva[1] I.Y. The experimental investigation of the neodymium speciation in the water vapor

[1] M.V. Lomonosov Moscow State University, Department of Geology, Moscow
[2] V. I. Vernadsky Institute of Geochemistry and Analytical Chemistry RAS, Moscow

Abstract. New experimental data on the speciation of neodymium in the water vapor under hydrothermal conditions are presented.

Key words: hydrothermal process, speciation of rare earth elements, neodymium, water vapor.

Neodymium is usually associated with elements with low volatility, since its oxide has low fugasity in vacuum [Kazenans, Chizhikov, 1976]. However influence of other components such as water, chlorine or fluorine can increase the amount of matter which can be transported by gas. This effect has been noticed in such low-volatile elements as gallium, silver, gold, copper and others [Pokrovski et al., 2013]. These days there are evidences of the gaseous transport of rare earth elements (REE) under hydrothermal conditions. According to the article [Gilbert, Williams-Jones, 2008], there are data of encrustations enriched by REE from actively degassing fumaroles of natrocarbonatite volcano Oldoinyo Lengai, Tanzania, which were products of dissipation from volcanic gases. In addition, concentrations of REE and yttrium were analyzed in high enthalpy fluid of Larderello-Travale geothermal field, Tuscany (Central Italy) [Möller et al., 2003], where the abundance of REE range from 0.1 to 10

pmol/kg, also distribution factors between HEF and source rocks were defined.

Two methods have been used to study the solubility in the gaseous phase of $Nd(OH)_3$ and Nd_2O_3: statically in autoclaves and dynamically by the flow method. Analyze of literature showed that for combination of lanthanides and water both oxide Ln_2O_3 and hydroxides $LnOOH$, $Ln(OH)_3$ can be stable [Viswanathiah et al., 1980, Shafer, Roy, 1959]. In case of neodymium under conditions of our experiments hydroxide $Nd(OH)_3$ has to be stable. Synthesis of stable phase was conducted according to the methods, stated in following articles: [Kutty et al., 1978; Viswanathiah et al., 1980]. Oxide Nd_2O_3 with stamp HO-E (OCT 48-197-81) was the initial phase. For obtaining the hydroxide the oxide powder was placed into autoclave with previously calculated amount of distilled water without CO_2 and was maintained under 400 ^{o}C and pressure 1 kbar during 15 days. Resulting phase was analyzed by X-ray powder diffraction, which confirmed that it is neodymium hydroxide $Nd(OH)_3$.

Experiments of neodymium transportation have been conducted through the use of static method in autoclaves under 200, 250 °C and pressure ranges from 3 to 15 and from 5 to 38 bar respectively (without reaching the saturation of the water vapor). The preparing of the experiment included volume calibration and lining of the autoclaves, calibration of the oven and preliminary calculations.

Before the experiment the definite amount of double distilled water was poured, this water set the pressure, which created only gaseous phase without liquid under experiment conditions. The pressure and density of saturated water vapor was taken from [Naumov et al., 1971]. Then the open titanium vial on the holder with the neodymium hydroxide was placed into the autoclave.

Autoclaves was maintained in the air thermostat SNOL-3.5 with fluctuation of the temperature ±1°C. The temperature was controlled by chromel – alumel thermocouple, duration of the experiments was 7 days.

During the experiment the water evaporated and the vapor interacted with solid phase in the vial. Components transported in the gaseous phase precipitated on the bottom and wall of the autoclave after the quenching (30-40 min in the reservoir with cold running water). After these operations the autoclave was opened and the vial with the neodymium hydroxide was retrieved. Washings were performed with a 10 ml of 3% solution HNO_3 under 200 °C to determine the amount of transferred material. Then autoclaves washing was repeated to determine the completeness of the operation.

The flow method has been used for exploration of Nd_2O_3 solubility in water vapor under 300, 350, 450°C and pressure ranges from 0.025 to 0.7 bar. The air flow, which speed was measured, passed through the two bubblers (with NaOH and water), which were placed in thermostat. There was the removal of carbon dioxide in the first bubble and the saturation of the water vapor under thermostat temperature in the second one. Thus the air flow of certain humidity has been forced through the quartz tube in the oven with Nd_2O_3 (stable phase under these conditions) under the operating temperature 300, 350 or 450ºC, where there was a reaction of the solubility of the neodymium in the gaseous phase. The glass filter at the tube end delayed aerosol particles of neodymium oxide.

As a result, the gas saturated with species, which can migrate in the vapor passed through the 3% solution of HNO_3 and the neodymium was trapped.

The solutions, which had been obtained by both methods were analyzed by ICP-MS (ELEMENT 2, Thermo Finnigan). The background solution was HNO_3 with concentration 3%. Indium with concentration 10 mcg/kg was added to the samples to control the intensity of sample supply. Solutions for calibration was prepared from standart solution for 69 elements of «Merk» company by serial dilution. ICP-MS data were calculated to the concentrations using methods, which were developed in Laboratory of the experimental geochemistry in Lomonosov Moscow State University.

The results of static experiments in the autoclaves demonstrated that the solubility of $Nd(OH)_3$ in water vapor doesn't depend on the water pressure, hence the proposed reaction is as follows:

$Nd(OH)_3$ (solid) = $Nd(OH)_3$ (gas).
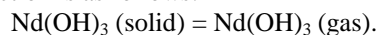
The logarithms of the equilibrium constants are 9.15±0.42 for 200 ºC and -9.30±0.31 for 250ºC.

In case of dynamic flow system experiments the solubility of Nd_2O_3 increases with water fugacity rising at all temperatures and the slope approximates 1.5. Thus, there can be assumed following reaction:

$0,5\ Nd_2O_3$ (solid) + $1,5\ H_2O$ (gas) = $Nd(OH)_3$ (gas).
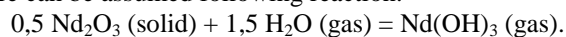
The logarithms of the equilibrium constants for the reaction are 8.31±0.42 for 300 ºC, -7.74±0.31 for 350 ºC and -7.03±0.61 for 400 ºC.

References:

1. Gilbert C.D., Williams-Jones A.E. 2008. Vapour transport of rare earth elements (REE) in volcanic gas: Evidence from encrustations at Oldoinyo Lengai. *Journal of Volcanology and Geothermal Research*.Volume 176, Issue 4, 15 October 2008, Pages 519–528.
2. Kazenans E.K., Chizhikov D.M. 1976. The pressure and composition of the vapor of the oxides of chemical elements. Moscow, «Nauka», 344-p. (rus).
3. Kutty T. R. N., Viswanathiah M. N., and Tareen J. A. K. 1978. Hydrothermal equilibria in $Nd_2O_3-\ H_2O-\ CO_2$ system //*Proc. - Indian Acad. Sci., Sect. A*, 87(4) 69-74.
4. Möller P., Dulsky P., and Morteani G. 2003. Partitioning of rare earth elements, yttrium, and some major elements among source rocks, liquid and vapor of Larderello-Travale Geothermal Field, Tuscany (Central Italy). *Geochimica et Cosmochimica Acta*, Vol. 67, No. 2, pp. 171–183.
5. Naumov G.B., Ryzhenko B.N., Hodakovsky I.L. 19741. The handbook of thermodynamic quantities. Moscow, Atomizdat (rus).
6. Pokrovski G.S., Borisova A.Y., Bychkov A.Y. 2013. Speciation and Transport of Metals and Metalloids in Geological Vapors. Reviews in Mineralogy & Geochemistry. Vol. 76 pp. 165-218.
7. Shafer M. W., Roy R. 1959. Rare-Earth Polymorphism and phase equilibria in rare-earth oxide-water systems //*J. Am. Ceram. Soc*., 42 (11) 563-570.
8. Viswanathiah M.N., Tareen J.A.K., Narayanan T.R. 1980. Hydrothermal phase equilibria studies in Ln_2O_3-H_2O systems and synthesis of cubic lanthanide oxides // *Materials Research Bulletin*, Vol. 15, (7), pp.

9. Viswanathiah M. N., Tareen J. A. K., Kutty T. R. N. 1977. Hydrothermal equilibria in Ln_2O_3-H_2O systems for neodymium, samarium, ytterbium and yttrium // *Indian Miner*., 17, 54-59.

Kotelnikova[1]Z.A., Kotelnikov[2]A.R. Phase state of the KF–NaF–KCl-contained fluids under 700-800°C and *P*=2000 bar: systems I and II types from synthetic fluid inclusions in quartz study

[1]Institute of Geology of Ore Deposits, Petrography, Mineralogy, and Geochemistry, RAS, Moscow

[2]Institute of Experimental Mineralogy RAS, Chernogolovka Moscow district

Abstract. Fluid inclusions in quartz were synthesized by the method of crack healing at 2 kbar and temperatures of 700, 750, and 800°C from solutions containing KF, NaF, KCl. The microthermomemtric study of the synthesized inclusions showed that under experimental conditions the fluid was heterogeneous and did not remain inert with respect to quartz. Some inclusions contained a glass-like phase, and liquid released from this phase by heating. Having been heated, some inclusions revealed liquid immiscibility.

Key words: synthetic fluid inclusions, liquid immiscibility.

The presence of fluorine exerts a significant influence on mass transfer and the entire course of mineral formation. Properties of fluorine-bearing fluids are still not adequately understood. The most common components in natural fluids are chlorine, sodium and potassium. Therefore, to simulate natural fluorinated fluids were selected solutions of fluorides and chlorides of these metals.

There are two types of phase diagrams for water-salt systems. In the binary phase diagrams of the first type, the critical curve does not intersect the solubility curve (three-phase equilibrium). In the phase diagrams of second-type systems, these curves meet at two points, P and Q, which are referred to as the lower and upper critical points, respectively. Critical phenomena occur in saturated solutions.

The H_2O–NaF system was investigated using synthetic fluid inclusions in quartz. It appeared that NaF – bearing fluid actively interacts with quartz at high temperatures and pressures, and quartz dissolves incongruently. The resulting intermediate compounds were observed in synthetic fluid inclusions as a crystalline phase, probably malladrite Na_2SiF_6, and a phase conventionally referred to as glass, because the boundary between this phase and liquid and gas is a regular meniscus.

The phase diagram of the H_2O–NaF system is of the second (or P–Q) type. The phase diagram of the system H_2O–KF belongs to the first type. Similar diagrams are characteristic of the solutions NaCl and of many other salts, which show a positive temperature coefficient of solubility. System H_2O–KF is poorly studied. The maximum temperature at which the research experiments have been ever conducted correspond to the values of 500°C, the maximum pressure – 190 bar. The authors commonly attribute this system to the systems of first type

without liquid separation. The temperature of the triple point of this system is 856°C, the eutectic is -21.8°C. Eutectic mixture is characterized by ice and KF•$4H_2O$ presence. Multiple peritectic points with equilibrium of vapor liquids and solid crystallohydrates KF with a different number of water molecules are observed on the state diagram. Solubility of the salt being significant at room temperature (near 47 mass % according to different authors) rises at higher temperatures. There are no data on the phase state of the solution at higher temperature and pressure. Since the increase in pressure prevents heterogeneity we can assume that analogously to the system H_2O-NaCl at 2 kbar and temperatures of 700–800°C, fluid remains homogeneous. However, the high reactivity of the KF can lead to interaction of quartz (and other silicates) with water-salt fluid. As a result, chemical compounds may produce water solutions with liquid separation on the phase diagram, for example, gieratite K_2Si_6 or different potassium silicates. In order to determine the phase state of the fluid, experiments were conducted by healing cracks in quartz in 0.5M solution of KF (2.9 wt. %) at 2 kbar and temperatures of 700, 750 and 800°C.

After experiments at 700°C two-phase inclusions, containing the liquid, vapor and homogenized liquid at 388–390°C, have been detected. According to cryometry results concentrations of salt in them are 2.8–3.0 wt. % KF. Composition of the inclusions corresponds to the initial content of the KF solution. The above facts indicate a homogeneous state of fluid under experiments conditions. There is no reason to assume chemical interaction silicate + fluid.

When 0.5M solution of KCl added to a solution of KF, fluid becomes heterogeneous. At that case experimental conditions are close to the critical point: the inclusion homogenized in liquid, vapor, and with critical phenomena at 369–393°C.

In the sample from experiments at 750°C with KF solution in addition to two-phase (liquid + vapor) inclusions, few inclusions containing glassy phase (Gl) at room temperature were observed in the sample. This phase does not freeze under cooling. During heating up to 450°C this phase does not change too. Further increase of temperature leads to a decrepitation of inclusions. In general, the appearance of two types of inclusions can be caused by: a) the heterogeneity of fluid and b) a change in the overall composition of the fluid as a result of the chemical interaction of silicates and water-salt fluid. Since it is assumed that the system H_2O–KF corresponds to first type systems without liquid separation, immiscible phases are vapor and liquid in heterogeneity. In this case, inclusion, capturing pure portions of these phases must be homogenized, respectively, in the vapor and liquid. Nevertheless, in the sample there are no inclusions with predominance of the gas phase. All two-phase inclusions homogenized in liquid over a wide temperature range, particularly: 366–375 (15 measurements) and 401–407 (3 measures). The process of homogenization was close to critical: the phase boundary changed its position slightly when heated, and then almost immediately disappeared. Cryometry of the inclusions was obstructed by the strong darkening, but the measured melting temperature of ice in all cases corresponds to concentrations of 0.9–2.5 wt. % KF. The above results of micrometric studying lead to the

following conclusions. It can be assumed that the fluid in the experience was homogeneous. In contrast to the experiment at 700ºC, the water-salt fluid at a temperature of 750ºC was chemically active relative to silicates, and as a result of chemical reactions part of KF was used. In this case, at different stages of experiment inclusions consistently were formed. They reflected the changes in the composition of the fluid. And, some of them captured the products of interaction in the form of glassy phase. Heterogenization of fluid was more productive for chemical interaction of fluid-silicate than heating: due to the high temperature hydrolysis the immiscible phases can differ significantly on their acid-base properties and react with silicates.

The chemical interaction of the water-salt fluid with quartz are marked in the products of all of experiments when a KCl add to fluid-making mixture. As a result glassy phase is fixed in the inclusions. The results of the cryometry indicate a significant shifting composition of the solution and the formation of substances with a negative temperature coefficient of the solubility. If we compare the results of experiments conducted at 750ºC, but with different ratios of salts KF and KCl in the initial solutions, we note the following. With the predominance in solution KCl (X_F^{fl}=0.25) fluid at experimental conditions was homogeneous. Some inclusions present with glassy phase. Heterogeneous conditions exist at case of increasing of the molar fraction of fluorine in the fluid to a value of 0/5 and the same concentration of KCl in the initial solution (1.9 mass %). Two- and three-phases inclusions are present in the sample. It should be noted that both the salts included in the fluid are compounds whose solubility is increased upon heating and aqueous solutions which have a first type of state diagram. Nevertheless in same case solid phases were detected in inclusions whose solubility decreases with increasing temperature. It is a feature of the second salt (P–Q) type. These observations lead the conclusion that during the experiment the fluid has changed its composition, which could occur only as a result of its interaction with quartz. It is possible that the glassy phase is also formed in this chemical interaction, although the emergence of such compounds is possible without the participation of salts in the system H_2O–SiO_2.

Kotova N.P. Experimental study of Nb_2O_5 solubility in fluoride solutions at 550º C and 500 bar

Institute of Experimental Mineralogy RAS, Chernogolovka Moscow district

Abstact. Niobium oxide solubility was investigated in HF and KF solutions ranging from 0.1 to 2 m at 550 °C and 500 bar (Co-CoO buffer). It is established that decreasing fluid pressure from 1000 to 500 bar in HF solutions virtually no effect on Nb2O5 solubility. In 0.01 m KF solutions the concentration of Nb decreases by about one order of magnitude and in 0.1 m KF solutions by 0.5 order with decreasing fluid pressure from 1000 to 500 bar. In 2 m KF solutions the concentration of Nb approaches 10-1.5 m that is quite enough for actual mass transfer of niobium by hydrothermal solutions.

For many years, we conducted comprehensive experimental and field geological studies aimed at obtaining quantitative estimates of the physico-chemical conditions of formation greisen and albitite deposits of W, Mo, Sn, Ta, Nb, and Li, associated with standard calc-alkaline, including the Li-F granites. In spite great advances of geologists in the study on mineralized granites and associated with greisen, albitite and other genetic types of rare metal deposits, many principle questions of their genesis still remain not clear.

The most accepted is genetic conception by V.I. Kovalenko [1977], consisting in the fact that rare metal Li-F granites are formed by crystal fractionation of the usual granitic magma under specific conditions, providing stage accumulation of flux elements such as F or Li and transition metal cations such as Nb and Ta in the residual melt.

However, for modeling of the formation conditions of tantalum deposits is necessary take into account also the role of hydrothermal-metasomatic processes [Beus et al, 1962]. The results of our experimental studies [Kotova, 2013] under P-T and solution composition conditions corresponding to the physicochemical parameters present during postmagmatic hydrothermal processes may provide some new criteria and restrictions on the interpretation of geological data and estimate the validity of one or another hypothesis of the genesis of rare metal deposits in granites.

The solubility of niobium oxide (Nb_2O_5) - analog of the natural mineral nioboksid as a function of the total fluoride concentrations has been investigated at T = 550 ° C, P = 500 bar in aqueous solutions of HF and KF with concentrations of 0.01; 0.1; 0.3; 1.0 and 2.0 mol / kg H_2O in the presence of oxygen buffer Co-CoO. Run duration was 18 days. A sealed-capsule quench technique was employed. Experiments were performed on high pressure hydrothermal apparatuses. The capsules and the container with buffer were sealed into cold-seal pressure vessel of Tuttle type with big working volume that gives possibility to isolate the capsules from the container with buffer. The same technique was used to study Ta_2O_5 solubility in fluoride and chloride solutions.

Solid run products were separated from the solutions by centrifugation method. After that the quenched aqueous solutions were analyzed by ICP/MS (Inductively Coupled Plasma Mass Spectrometry) and ICP/AES (Atomic Emission Spectroscopy) procedures for Nb, Ta, Mn, and Fe and admixture elements: Ti, W, Sn, K, and Na.

To control congruent or incongruent dissolution of Ta oxide and to determine chemical composition of newly-formed phases (in case of their manifestation) the initial materials and solid run products were studied by X-ray diffraction, and electron microprobe analysis (Cam Scan MV 2300 (VEGA TS5130MM).

The experimental data are shown in Fig. 1 and 2. It was found that the dependence of Nb_2O_5 solubility on fluoride concentrations follows linear trends in HF and KF solutions for all conditions considered.

It is established that decreasing fluid pressure from 1000 to 500 bar in HF solutions virtually no effect on Nb_2O_5 solubility. At low HF concentrations (less than 10^{-2} m) niobium content is 10^{-3} m. With increasing F- ion

concentration Nb_2O_5 solubility strongly increases and at high HF concentration (1m and higher) reaches significant values 10^{-2}–$10^{-1.5}$ m that is quite enough for actual mass transfer of niobium by hydrothermal solutions.

The experimental data show similarities in Nb_2O_5 solubility in HF and KF solutions of low concentrations (0.01 and 0.1 m) at T = 550 ° C and P = 1000 bars. However, unlike HF solutions, in 0.01 m KF solutions the concentration of Nb decreases by about one order of magnitude and in 0.1 m KF solutions by 0.5 order with decreasing fluid pressure from 1000 to 500 bar.
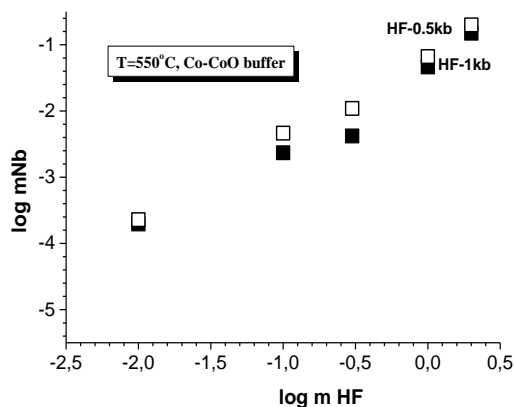

Fig.1. Effect of HF concentration and fluid pressure on the Nb_2O_5 solubility at T = 550 ° C (squares-at P = 0.5kbar, filled squares–at P=1kb)

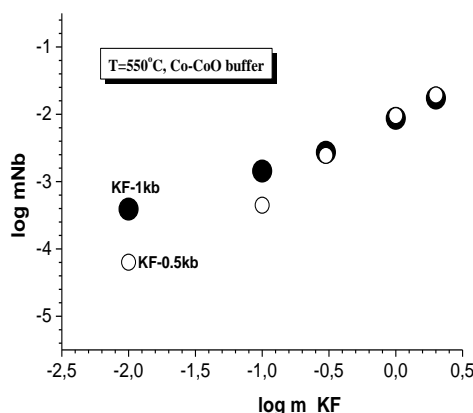**Fig. 2.** Effect of KF concentration and fluid pressure on the Nb_2O_5 solubility at T = 550 ° C (circles-at P = 0.5 kbar, filled circles-at P = 1kb)

According to results of X-ray diffraction at low HF concentration niobium oxide dissolves congruently (without the composition changing). At high HF concentration niobium oxide has an incongruent solubility. The crystals of niobium oxide fluoride with the formula Nb_3O_7F, belonging to the orthorhombic system, are formed.

In 0.01 m KF solution niobium oxide dissolves congruently. In KF solutions of higher concentration niobium oxide dissolves incongruently. In this case, in 0.1 m KF solution niobium oxide is replaced by oxyfluoride of potassium type $KNb_6O_{15}F$, belonging to the monoclinic crystal system. In 0.3, 1 and 2m KF solutions potassium-

niobate $K_2Nb_4O_{11}$ is formed, which belongs to the tetragonal system.

This study demonstrates that Ta and Nb can be transferred hydrothermally in the amounts sufficient for the formation of commercially viable ore deposits via concentrated fluoride solutions. P-T conditions have little influence on the solubility of niobium and tantalum.

References:

1. Kovalenko V.I. (1977). Petrology and geochemistry of rare metal granitoids: Akademiia Nauk SSSR, Sibirion Devision, Novosibirsk (in Russian)

2. Beus A.A., Severov E.A., Sitnin A.A., Subbotin K.D. (1962). Albitized and greisenized granites (apogranites), Akademiia Nauk SSSR, Moskva, 196 p

3. Kotova N.P. (2013). Experimental study of temperature dependence of niobium oxide solubility in fluoride solutions in connection with genesis of tantalum deposits. Eksperimetalnaya geokhimiya, T.1, N 3, URL: http://exp-geochem.ru/JPdf/03_2013/ENG/13_03_2013_Eng.pdf.

Redkin A.F.,Kotova N.P. Experimental study of microlyte solubility dependence on NaF concentration in aqueous solution at 800°C and 200 MPa.

Institute of Experimental Mineralogy RAS, Chernogolovka Moscow district

Abstact. New data are obtained on the microlite $(CaNa)Ta_2O_6F$ solubility in the $NaF-H_2O$ system of the P-Q type in a wide concentration range of sodium fluoride (from 0 to 40 wt. % NaF) at the indicated physico-chemical parameters. It is shown that the solubility data in the homogeneous region of $NaF-H_2O$ solutions can be described by three predominant particles – $Ta_2O_5°$, $Na_6H_2Ta_6O_{19}°$, and $NaHTaO_3F°$, as in the experiments at T = 800°C and P = 230 MPa [Redkin, Kotova, 2013]. At the transition to the immiscibility region there is anomalous behavior of the microlite solubility curve associated with the separation of the solution into two fluid phases (L_1 and L_2) of different acidity. For the first time, the NaF concentrations were evaluated in the L_1 (5 ± 1 wt. %) and L_2 (25 ± 1 wt. %) fluid phases at 800°C and a total pressure of 200 MPa.

Key words: experiment, microlite, immiscibility region

The solutions of the P-Q type in the immiscibility region at high T-P parameters are of interest as the solvents of ore components because they form a couple of fluid phases (L1 and L2), significantly differing in the salt content and, respectively, the dissolving ability in respect of ore components. Therefore, the study of such systems is of great scientific and practical interest.

The aim of our research is to estimate the NaF concentration of $NaF-H_2O$ solution in the L_1 and L_2 fluid phases in the immiscibility region at the specified physicochemical parameters. To achieve this purpose, we used the solubility method. The method consists in the fact that, as a result of studies of the NaF concentration effect on the solubility of microlite $(CaNa)Ta_2O_6F$ in the solutions of the P-Q type at T-P parameters above point Q, the region of fluid immiscibility in the $NaF-H_2O$ system

will be highlighted. Microlite contains NaF as minal and has a very low solubility in the fluoride solutions, which makes it very promising for this kind of research.

The feature of the water-salt systems of the P-Q type, such as NaF-H$_2$O and LiF-H$_2$O, is their high-temperature specificity at which the research methods, such as sampling of the individual fluid phases and in-situ analysis of fluid inclusions did not seem possible. The critical point Q for the NaF-H$_2$O system is at $T > 700°C$ and $P \sim 200$ MPa [Kotelnikova, Kotelnikov, 2010]. The immiscibility region is above this temperature. At these parameters, quartz has a rather high solubility in the water (1.5 wt.%) [Manning, 1991]). In the fluoride solutions the quartz solubility is even higher, which greatly complicates the investigated system.

Experiments were performed on a high-pressure hydrothermal line at 800°C and $P = 200-230$ MPa. Run duration was 7-9 days. Starting material was microlite (Mic) - (CaNa)Ta$_2$O$_6$F, obtained by hydrothermal synthesis at 800°C and $P = 200$ MPa in 1 M NaF solution: NaF (of high purity), CaF$_2$ (of high purity) and tridistilled H$_2$O. The charge of solid starting materials (10-15 mg of pyrochlore, 0-5 mg of CaF$_2$, from 0 to 100 mg of NaF) and 0.15 ml of H$_2$O were sealed into Pt capsules. Run products were analyzed by means of XRD, REM (CamScan, Vega-II), ICP-AES, and ICP-MS methods. According to the results of XRD and REM analyses, there were microlite and very minor amounts of fluorite and villiaumite in the solid products of the runs. The studies were carried out in two homogeneous regions (HS-I-homogeneous solution of the low concentrations of NaF and HS-II-highly concentrated solution of NaF), and also in the immiscibility region of the fluid phases of L$_1$ (moderate density fluid) and of L$_2$ (dense fluid), located between the HS-I and HS-II. The Ta concentration in HS-I and HS-II homogeneous solutions, saturated by Mic at constant P-T parameters, should be described by a continuous function:

$$m_{Ta} = \sum_i n \times m_i, \qquad (1)$$
$$m_i = F(K_p, m_{NaF}^k, X_{H2O}, m_{HF}^v)$$

where m_i - molal concentration of Ta in the form of particle i, which is a complex function of the equilibrium constant (Kp), molal concentration of NaF, HF, and the mole fraction of water in the corresponding exponents.

In the region of fluid immiscibility (from L$_1$ to L$_2$) the microlite solubility and the Ta mass concentration varies linearly from the mass concentration of NaF. According to the lever rule,

$$C_{Ta} = X_{L1} \times C_{Ta1} + X_{L2} \times C_{Ta2}, \qquad (2)$$

where the X_{L1} and X_{L2} are mass fractions of L$_1$ and L$_2$ fluid phases, C$_{Ta1}$ and C$_{Ta2}$ are mass concentrations of Ta in the L$_1$ and L$_2$ phases, respectively. After transformation,

equation 2 takes the form of a linear function from the mass concentration of NaF (C$_{NaF}$):
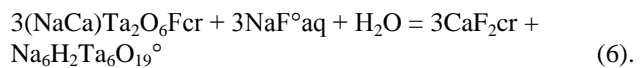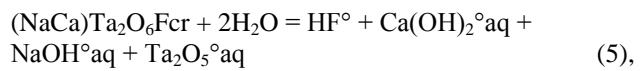
$$C_{Ta} = A \times C_{NaF} \times (C_{Ta1} - C_{Ta2}) + B \times (C_{Ta1} - C_{Ta2}) + C_{Ta2}, \qquad (3)$$

where $A = 1/(C_{L2} - C_{L1})$ и $B = C_{L2}/(C_{L2} - C_{L1})$ - constants depending only on the mass concentrations of NaF in L$_1$ (C$_{L1}$) and L$_2$ (C$_{L2}$) phases, respectively.
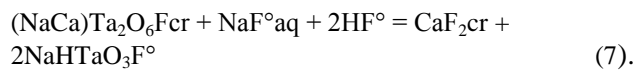
The results of analyses of the solutions after experiments on microlite solubility at 800°C, $P = 200$ MPa in comparison with the previously published data [Redkin, Kotova, 2013] at 800°C, $P = 230$ MPa are shown in Fig. 1. The trend of change of mTa from mNaF and the mole fraction of water X(H$_2$O) in the regions of homogeneous solutions of HS-I and HS-II corresponds to the equation

$$m\text{Ta} = 2.14 \times 10^{-6} + 9.2195 \times 10^{-9} \times (m\text{NaF})^3 \times \text{X(H}_2\text{O)} \qquad (4)$$

and reactions

$$\text{(NaCa)Ta}_2\text{O}_6\text{Fcr} + 2\text{H}_2\text{O} = \text{HF}° + \text{Ca(OH)}_2°\text{aq} + \text{NaOH}°\text{aq} + \text{Ta}_2\text{O}_5°\text{aq} \qquad (5),$$

$$3\text{(NaCa)Ta}_2\text{O}_6\text{Fcr} + 3\text{NaF}°\text{aq} + \text{H}_2\text{O} = 3\text{CaF}_2\text{cr} + \text{Na}_6\text{H}_2\text{Ta}_6\text{O}_{19}° \qquad (6).$$

In the immiscibility region the increase in solubility in the phase L$_1$ and its decrease in the phase L$_2$ is connected with the reaction (7)

$$\text{(NaCa)Ta}_2\text{O}_6\text{Fcr} + \text{NaF}°\text{aq} + 2\text{HF}° = \text{CaF}_2\text{cr} + 2\text{NaHTaO}_3\text{F}° \qquad (7).$$

The composition of the Ta^{5+} complexes in the neutral and weakly alkaline solutions of NaF was discussed earlier [Redkin, Kotova, 2013]. According to data obtained, there is not observed the formation of the Na$_2$Ta$_2$O$_6$°aq particles in the HS-I region, that seems to be the case due to insufficient amount of experimental data at low concentrations of NaF. In the range of the NaF concentrations from 5 to 25 wt. % (Fig. 1), an anomalous change of microlite solubility is observed, which is associated with the transition from the homogeneous region to immiscibility one in the NaF-H$_2$O system. This indicates that the region of immiscibility at 800°C, $P = 200$ MPa is limited by the NaF concentrations: 5 ± 1 wt. % (L$_1$) and 26 ± 1 wt. % (L$_2$). We note that in the runs at 800°C, $P = 230$ MPa the L$_1$ and L$_2$ fluid phases contained 12 ± 1 and 25 ± 1 wt. % NaF, respectively.

Thus, for the first time by the solubility method of poorly soluble mineral (microlite) there were estimated the NaF concentration at 800°C, $P = 200$ and 230 MPa in the L$_1$ and L$_2$ phases in the region of fluid immiscibility in the NaF-H$_2$O system at 800°C, $P = 200$ and 230 MPa.
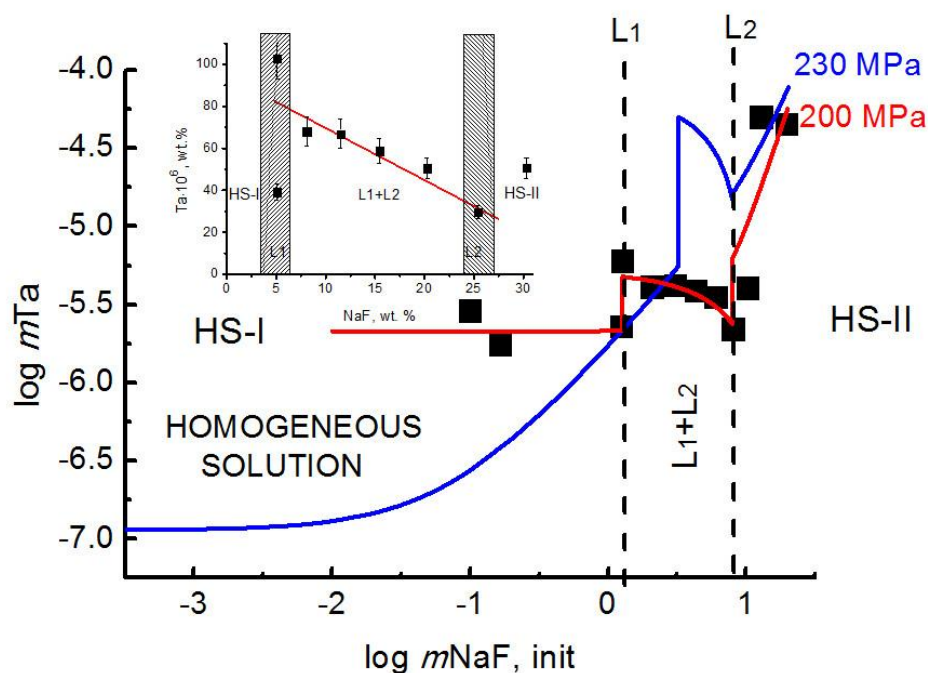
Fig. 1. Results of the runs on the microlite (NaCa) Ta$_2$O$_6$F solubility in the NaF solutions at 800°C, P = 200 MPa. Colored lines show the trends of changes of mTa from mNaF at 800°C, P = 200 MPa (red) and P = 230 MPa (blue) [Redkin, Kotova, 2013]. Symbols: HS-I - homogeneous solution at low concentrations of NaF, HS-II is a homogeneous solution at high concentration of NaF, L$_1$ + L$_2$ is the immiscibility region of fluid phases in the NaF-H$_2$O system.

References

1. Redkin A.F., Kotova N.P. (2013): Experimental study of microlite solubility dependence on NaF concentration in aqueous solution at 800°C and 230 MPa // *Experimental Geochemistry*. V. 1. No. 3. URL: http://exp-geochem.ru/JPdf/03_2013/ENG/16_03_2013_Eng.pdf
   Redkin A.F., Kotova N.P. (2013): Experimental study of microlite solubility dependence on NaF concentration in aqueous solution at 800°C and 230 MPa. *Experiment in Geosciences*. V. 19. No 1. P. 92-93.
2. Kotelnikova Z.A., Kotelnikov A.R. (2010): Experimental study of heterogeneous fluid equilibria in the silicate – salt - water systems // Geology of Ore Deposits. V. 52. N 2. P. 171-185.
3. Manning C.E. (1994): The solubility of quartz in H$_2$O in the lower crust and upper mantle // *Geochim. Cosmochim. Acta*. V. 58 (22). P. 4831-4839.

Tauson V.L. and Kravtsova R.G. Structurally and superficially bound noble metals in ore minerals: Experimental and natural evidence

A.P.Vinogradov Institute of Geochemistry SB RAS, Irkutsk

Abstract. Using the combination of local analytical methods (ICP MS-LA, AFM, SEM) and the method of statistical samplings of analytical data for single crystals (SSADSC), the evidence of the permanent presence of two binding forms of noble metals (Au, Pt, Pd) in ore minerals is obtained. These are the structurally and superficially bound forms observed in both experimental and natural systems – in minerals of gold ore deposits of different genetic types. The consequences of this phenomenon for the theory of ore-forming processes and practical aspects of exploration and recovery of ore objects are considered.

Key words: pyrite, arsenopyrite, magnetite, gold, palladium, platinum, distribution, hydrothermal systems, gold ore deposits.

Introduction. The present-day studies using modern surface-sensitive methods provide evidence of the existence of nanometer-sized objects occupying the surfaces of hydrothermally synthesized and naturally occurred ore minerals [Tauson et al., 2008; 2012, 2014a]. Their composition is strongly dependent on physicochemical parameters of the environment so being the typomorphic feature for certain conditions of mineral formation. The most evident peculiarity of such superficial nano-sized phases (SNP) is their ability to take up the incompatible elements, particularly, the noble and rare metals with high accumulation coefficients (more than 1000 relative to crystal volume). This effect involves the compatible (true isomorphic) elements as well providing ten-to-hundred-fold rise to their contents in the surface layer of a crystal. At the moment, it is important to appreciate the consequences of this phenomenon for the mechanism of concentration of noble and rare metals in geochemical systems and define its genetic significance and possible implications for practice.

Experimental and analytical methods. Ore mineral crystals (pyrite, As-pyrite, magnetite, Mn-magnetite, hematite) doped with noble metals (NM) were synthesized by the method of thermogradient hydrothermal synthesis in solutions contained ammonium chloride. The experiments were performed at 450 and 500°C and 1 kbar (100 MPa) pressure and provided sampling of a portion of fluid phase. As NM are incompatible in most of minerals of ore deposits, the processes of their fractionation and concentration cannot be sufficiently characterized without quantitative estimates of dual distribution coefficients. Duality means that two components of the distribution coefficient exist – one refers to the structural impurity and obeys Henry's law, another refers to non-structural mechanism of the element uptake, first of all, the surface enrichment. The surface is an irremovable and widespread crystal defect. The methods applied for the analyses of run

products (crystals and trapped fluid phase) were the following: atomic absorption spectrometry (particularly SSADSC version, the statistical samplings of analytical data for single crystals), mass spectrometry with inductively coupled plasma and laser ablation (ICP MS-LA), atomic force microscopy (AFM) and scanning electron microscopy (SEM). The analytic devices of IGC SB RAS (spectrophotometers "Perkin-Elmer" models 503 and AAnalyst-200, quadruple mass-spectrometer Perkin Elmer NexION 300D and laser ablation platform NWR-213, scanning probe microscope SMM-2000) and LI SB RAS (scanning electron microscope FEI Company Quanta 200) were used. The comparison of the results obtained with SSADSC and ICP MS-LA is a subject of much methodical interest. The first method may be designated "semi-local" in the sense that it can characterize a sample as a whole and comparable with both bulk analysis and local analysis (because it takes account of the forms of the element occurrence). The second one is essentially local and its results are strongly dependent of the point coordinate as also in the case of the electron probe microanalysis [Pavlova, Anchutina, 2013].

Natural objects. We have studied 38 samples of pyrite from 12 gold ore deposits of different genesic types within the gold-bearing provinces in East Siberia, North-East Russia, Far East Russia, Uzbekistan with SSADSC method. More than 3000 single crystals were analyzed providing the statistical reliability of the results. The sporadic study of other ore minerals were performed with arsenopyrite, galena and magnetite. The crystals of arsenopyrite of Natalkinskoe deposit (North-East Russia) were studied with ICP MS-LA.
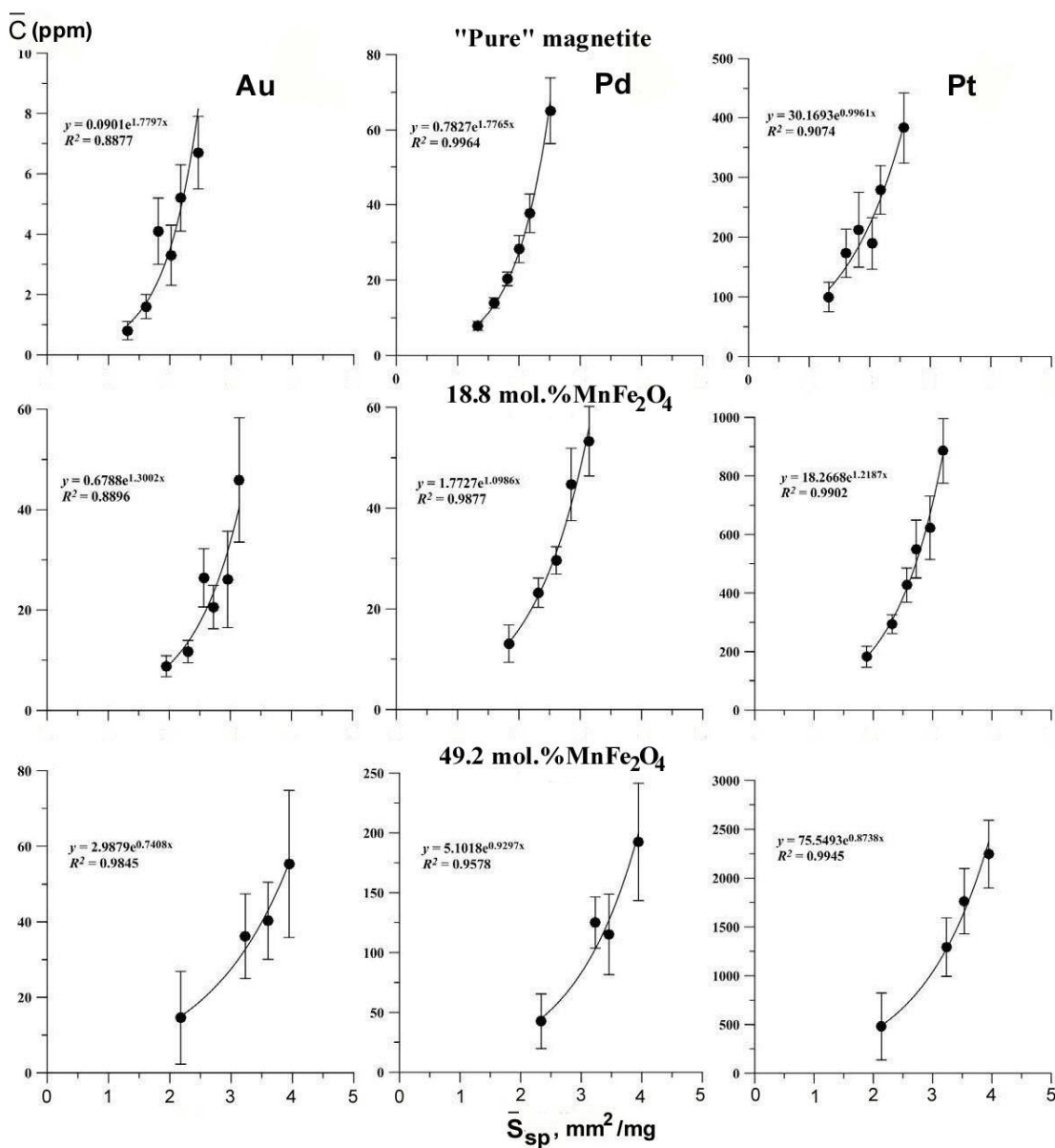

Fig. 1. Dependences of the average contents of uniformly distributed NM on the specific surface area of the average crystal in the size fraction for the crystals of magnetite and Mn-magnetite synthesized at 500°C. *The preexponential factor indicates the content of structurally bound NM. The exponential power index characterizes the contribution of superficially bound forms.*

Experimental results. Dependences of the average contents of uniformly distributed NM (Au, Pd, Pt) in magnetite and manganomagnetite on the specific surface area of the average crystal in the size fraction are expressed by highly determinate exponents (Fig.1, R^2=0.89-0.99). The similar situation was previously reported for Au in pyrite, As-pyrite and magnetite [Tauson et al., 2011; 2012]. The contents of structurally bound forms of NM are significantly and regularly increase with manganese end member elevation in the interval from 0 to 49 mol.%. The concentration of structural Au elevates from 0.1 in "pure" magnetite up to 3 ppm in Mn-containing magnetite; structural Pd content increases from 0.8 to 5.1 ppm. The slope of exponents decreases indicating diminution of the contribution of structurally bound NM. This is supported with XPS and AFM data showing lesser development of oxyhydroxide SNP on the surface of high-manganous magnetite. This phase is responsible for the trace element uptake by the magnetite surface and has the approximate composition as the following:

$$Fe^{3+}_{1+x} Fe^{2+}_{1-x} \left[O^{2-}_{1+y} (OH)^{-}_{1-y} \right] V^{-}_{2-y+x},$$
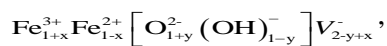
where V denotes Fe vacancy.

The spatial distribution of several trace elements has been studied with ICP MS-LA. The set of elements studied includes chromium which was added to the experiments in the form of potassium dichromate to enhance the magnetite growth process. The magnetite surface was not enriched with Cr in contrary to coexisting pyrite and pyrrhotite in sulfide system [Tauson et al., 2014b]. This is possibly due to the incompatibility of Cr in oxyhydroxide SNP. The latter, at the same time, readily absorbs Mn and a lot of other elements including NM and As (Fig. 2). The superficial phase is unstable under the laser beam, so it seems difficult or impossible to obtain precise data for the layer properly occupied by SNP ($\leq$300 нм). Taking advantage of a compatible Mn as a reference element, it can be shown that, to a first approximation, the element content in a superficial layer is $C^{sur} \sim C_{hLA} \cdot h_{LA}/h$, where h_{LA}=1.5 μm (average depth of burn groove of the surface layer), h=0.3 μm (thikness of SNP). The well-defined dependences of element concentrations on the specific surface area can be observed only in the case when SNP replicate the crystal habit (i.e. homothetic to it) and has a uniform thickness. It seems not improbable that the ratio of real and topological surface area affects the C^{sur} estimate but such effect is unnoticeable owing to small variations in roughness of crystal surface.
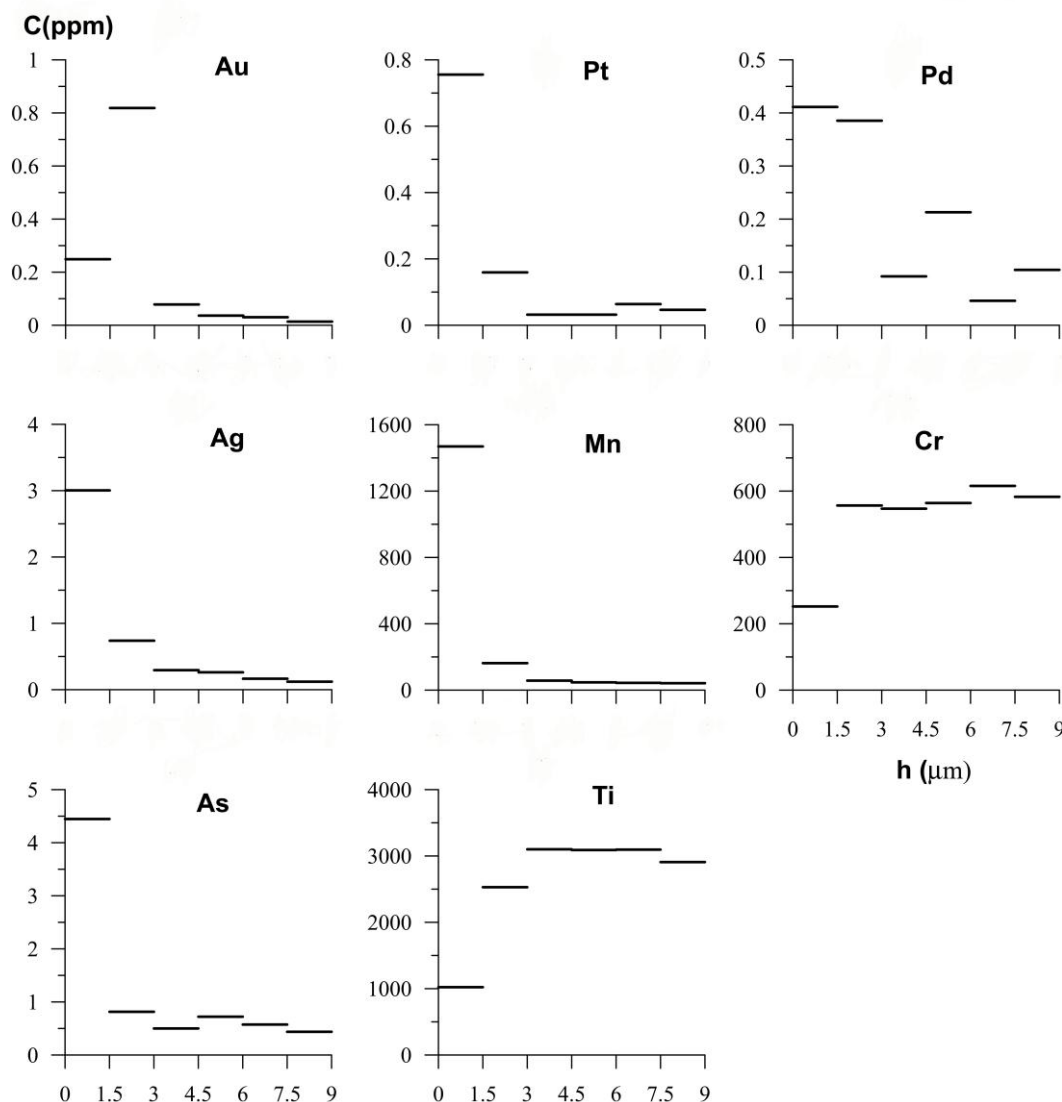

Fig. 2. Results of the layer-by-layer ICP MS-LA analysis of magnetite crystals (one pass-1.5 μm). Gap corresponds to average content in the interval respective.

Notice that all admixed elements except Cr and Ti (material of reaction vessel is titanium alloy) enrich the surface layer

The reason for the effect of NM concentration is the high values of the distribution coefficients for SNP (Table 1) sufficiently exceeding that ones for the structurally bound admixture. In the case of magnetite, D^{sur} elevation relative to D^{str} amounts 14 times for Au and Pt and 20 times for Pd. Notice that the data in Table 1 refer to a whole mass of the sample, not to a SNP. The NM contents in the latter reach $3\text{-}4\cdot10^3$ ppm.

Table1. Ratios of concentrations of structurally and superficially bound forms of NM in magnetite and Mn-magnetite and their distribution coefficients "mineral - hydrothermal solution"

Element	No. of experim.	C^{str}/C^{sur}	D^{sur}/D^{str}
Au	10	0.07 ± 0.03	14.3
Pd	9	0.05 ± 0.01	20
Pt	3	0.07 ± 0.03	14.3

Natural data. The application of SSADSC method to pyrites of gold ore deposits has shown that a sufficient part of Au is present as a superficially bound form. The proportion of structurally and superficially bound Au varies in wide range from ~0.00n-0.0n in pyrites from metasomatites formed during pre-ore stage of sulfidation of wall rocks up to ~0.n-1.3 in the ore-body pyrites [Tauson et al., 2014a]. The reason consists in the property of SNP to elevate the distribution coefficient "crystal-solution" as compared to bulk phase of pyrite due to a high absorption ability of the pyrrhotite-like nonautonomous phase on the pyrite crystal surface [Tauson et al., 2008]. Using experimentally determined distribution coefficient of the structurally bound Au between pyrite and hydrothermal solution [Tauson et al., 2011], Au contents in ore-forming fluids are estimated to be from 0.6 up to 50 ppm. The values obtained for black-shale formation have a propensity to the beginning of this interval whereas the values for epithermal gold-silver formation are concentrated within the middle and closer to the end of the interval. Highly determinate size dependences of uniformly distributed concentrations of Au in crystals are not an exclusive feature of pyrite. This can be exemplified with several ore minerals from gold ore deposits of Eastern Transbaikalia and East Sayan (Fig. 3). Despite the wide variations of Au content in size fractions (1-2 orders of magnitude), the contents of structurally bound form vary within the narrow limits (0.2-1.8 ppm). During the study of pyrites from the deposits of different genetic types not a case was marked when C^{str} appreciably exceeded 5 ppm, in accordance with the results on the incorporation limit of gold in hydrothermal pyrite - 3 ± 1 ppm [Tauson, 1999]. This demonstrates high possibilities of the SSADSC method.
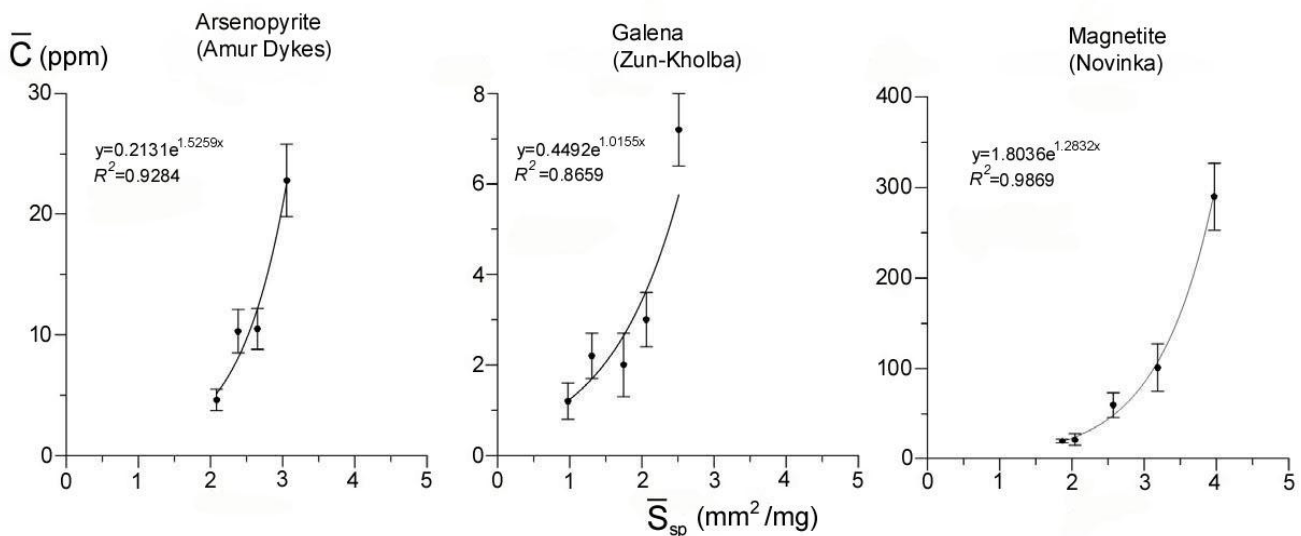

Fig. 3. Dependences of the average content of uniformly distributed Au on the specific surface area of the average crystal in the size fraction for three ore minerals.

The direct data on the enrichment of SNP with NM were obtained for arsenopyrite from the deposit Natalka with an ICP MS-LA method. It was proved to be possible to calibrate the depth of burn channel depth with AFM and get a detailed picture of the element distribution throughout the layer of approximately 600 nm thick (Fig. 4). Despite the reproducibility of the results leaves much to be desired, the data on the enrichment of layer ~100 or ~200 nm with NM was supported for a majority of the crystals studied as well as the presence of structural forms of NM in discernible concentrations.

Geochemical implications. (1) The studies of nonautonomous phases and surface layers of mineral crystals are firstly turn one's attention to the genetic aspects of nanomineralogy – typomorphism and typochemistry of nanosized components of mineral systems. (2) The emergence of new analytic techniques as ion-probe microanalysis, ICP MS with laser ablation, and nano-SIMS with the diameter of the incident beam of 50-100 nm gives possibility to revealing the fine elements of the zonality of ore mineral crystals in respect of trace elements. They are often identified with the peculiarities of the ore process, for instance, pulsating supply of fluid of different genesis – meteoric, magmatic or metamorphic – and different sources of metals – sedimentary-diagenetic or magmatic (mantle-core or mantle). The existence of

SNP enriched with incompatible elements brings cardinal changes to such interpretation. (3) Choosing the effective technology of ore processing and concentration it seems important to estimate the relation of the desired component to concrete structure element of the ore system determining the main parameters of the process – the extent of material reduction, the necessity and conditions of roasting, use of specific chemicals. It is important to be informed about how much and what elements could be lost into tailings with the fine fractions of concrete ore and vein minerals.
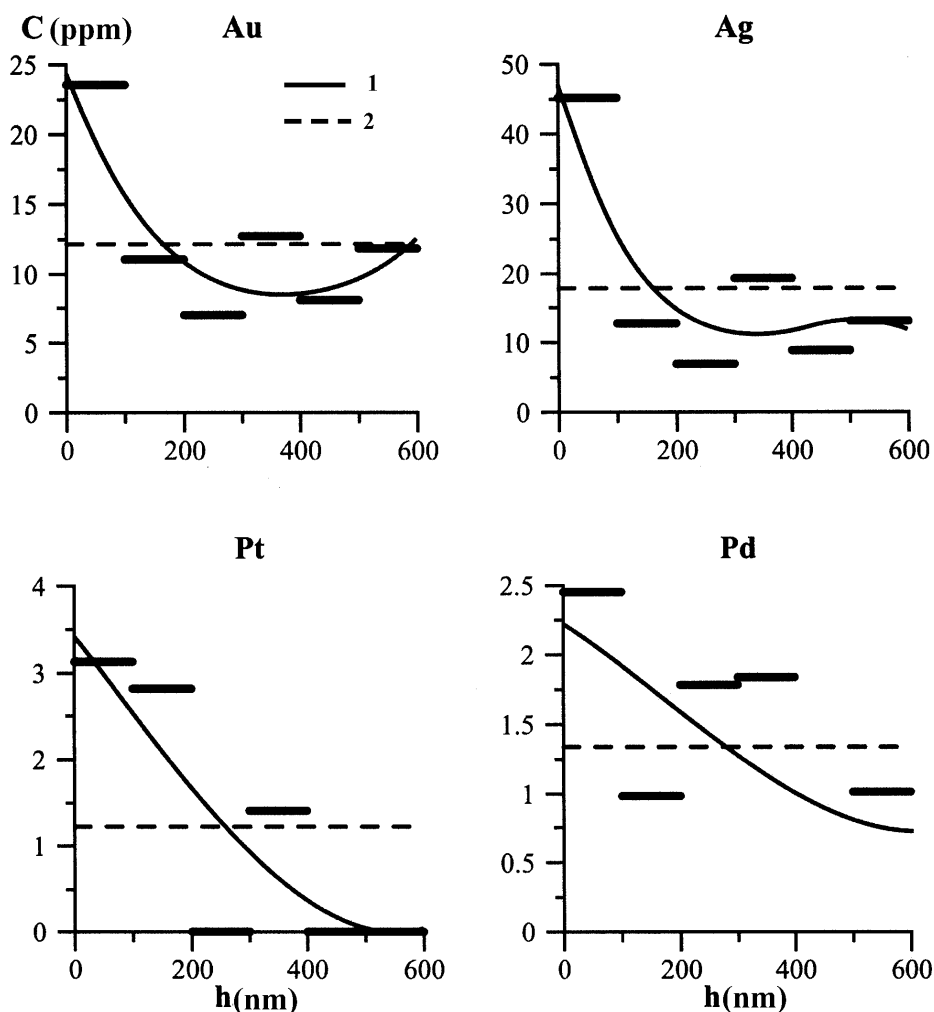

Fig. 4. Typical depth profiles of NM distribution in arsenopyrite crystal from Natalkinskoe deposit.

1 – average contents in the layers 0-100, 100-200 nm, etc.

2 – average content in the whole layer 0-600 nm.

References:

1. Pavlova L.A., Anchutina E.A. (2013). Standard sample of columbite-tantalite composition (CT-1) for electron probe microanalysis. *Zav.Lab. Diagn. Mater.*, v.79, no.8, p. 65-68.
2. Tauson V.L., Babkin D.N., Lustenberg E.E., Lipko S.V., Parkhomenko I.Yu. (2008). Surface typochemistry of hydrothermal pyrite: Electron spectroscopic and scanning probe microscopic data. I. Synthetic pyrite. *Geochem. Internat.*, v. 46**,** no.6, p. 565-577.
3. Tauson V.L., Babkin D.N., Pastushkova T.M., Krasnoshchekova T.S., Lustenberg E.E., Belozerova O.Yu. (2011). Dualistic distribution coefficients of elements in the system mineral-hydrothermal solution. I. Gold accumulation in pyrite. *Geochem. Internat.*, v. 49, no.6, p. 568-577**.**
4. Tauson V.L., Babkin D.N., Pastushkova T.M., Akimov V.V., Krasnoshchekova T.S., Lipko S.V., Belozerova O.Yu. (2012). Dualistic distribution coefficients of elements in the system mineral-hydrothermal solution. II. Gold in magnetite. *Geochem. Internat.*, v. **50**, no. 3, p. 227-245.
5. Tauson V.L., Kravtsova R.G., Smagunov N.V., Spiridonov A.M., Grebenshchikova V.I., Budyak A.E. (2014a). Structurally and superficially bound gold in pyrite from deposits of different genetic types. *Russian Geol. Geophys.*, v. 55, no. 2, p. 273-289.
6. Tauson V.L., Lipko S.V., Smagunov N.V., Arsent'ev K.Yu., Loginov B.A.(2014b). Influence of surface nanophases on the processes of crystal formation in multiphase mineral systems. *Dokl.Earth Sci.*, v. 455, part 1, p. 317-322.
7. Tauson V.L. (1999). Gold solubility in the common gold-bearing minerals: Experimental evaluation and application to pyrite. *Eur. J. Mineral.*, v.11. no. 6, p.937-947.